VIROLOGY

10.1126/sciadv.1501889

PPM1A silences cytosolic RNA sensing and antiviral defense through direct dephosphorylation of MAVS and TBK1

Weiwen Xiang,[1]* Qian Zhang,[1]* Xia Lin,[2] Shiying Wu,[1] Yao Zhou,[3] Fansen Meng,[1] Yunyun Fan,[1] Tao Shen,[2] Mu Xiao,[1] Zongping Xia,[1] Jian Zou,[3] Xin-Hua Feng,[1,2†] Pinglong Xu[1†]

Cytosolic RNA sensing is a prerequisite for initiation of innate immune response against RNA viral pathogens. Signaling through RIG-I (retinoic acid–inducible gene I)–like receptors (RLRs) to TBK1 (Tank-binding kinase 1)/IKKε (IκB kinase ε) kinases is transduced by mitochondria-associated MAVS (mitochondrial antiviral signaling protein). However, the precise mechanism of how MAVS-mediated TBK1/IKKε activation is strictly controlled still remains obscure. We reported that protein phosphatase magnesium-dependent 1A (PPM1A; also known as PP2Cα), depending on its catalytic ability, dampened the RLR-IRF3 (interferon regulatory factor 3) axis to silence cytosolic RNA sensing signaling. We demonstrated that PPM1A was an inherent partner of the TBK1/IKKε complex, targeted both MAVS and TBK1/IKKε for dephosphorylation, and thus disrupted MAVS-driven formation of signaling complex. Conversely, a high level of MAVS can dissociate the TBK1/PPM1A complex to override PPM1A-mediated inhibition. Loss of PPM1A through gene ablation in human embryonic kidney 293 cells and mouse primary macrophages enabled robustly enhanced antiviral responses. Consequently, Ppm1a$^{-/-}$ mice resisted to RNA virus attack, and transgenic zebrafish expressing PPM1A displayed profoundly increased RNA virus vulnerability. These findings identify PPM1A as the first known phosphatase of MAVS and elucidate the physiological function of PPM1A in antiviral immunity on whole animals.

INTRODUCTION

Metazoans use innate defense mechanisms to defend pathogen infections, by recognizing various conserved molecular motifs called pathogen-associated molecular patterns and initiating host defense countermeasures. In particular, viral double-stranded RNA (dsRNA) is sensed by cytosolic retinoic acid–inducible gene I (RIG-I)–like receptors (RLRs) (*1*–*3*) and membrane-bound Toll-like receptors, whereas viral DNA can be recognized by cGAS (cyclic adenosine 5′-monophosphate–guanosine 3′,5′-monophosphate synthase) (*4*–*7*), DAI {DNA-dependent activator of IRF [interferon (IFN) regulatory factor]} (*8*), RNA polymerase III (*9*), IFI16 (IFN-γ–inducible protein 16) (*10*), or DDX41 (DEAD-box helicase 41) (*11*). Facilitated by mitochondria-associated MAVS (mitochondrial antiviral signaling protein) (also known as VISA, IPS-1, and Cardif) or endoplasmic reticulum–associated STING (stimulator of IFN gene) (also known as ERIS, MITA, MPYS, or TMEM173), binding of viral dsRNA or DNA to cytosolic sensors leads to activation of Tank-binding kinase 1 (TBK1) and/or IκB kinase ε (IKKε), which phosphorylates and activates the signal mediator IRF3 (*12*, *13*).

Signal from RIG-I or MDA5 (melanoma differentiation–associated protein 5) to mitochondrial adaptor MAVS triggers activation of both TBK1/IKKε-IRF3 and nuclear factor κB (NF-κB) pathways (14–17). In receiving signals from RIG-I/MDA5, MAVS self-associates and polymerizes into three-stranded helical filaments on mitochondria, which serve as the platform to recruit TRAFs (tumor necrosis factor receptor–associated factors), TBK1/IKKε, and IRF3 to form functional signal complexes, eventually leading to IRF3 C-terminal phosphorylation and activation (*18*). Thus, MAVS is central to linking intracellular dsRNA detection to antiviral responses and is critical for creating antiviral cellular state. Activated IRF3 dimerizes and translocates to the nucleus and acts as a DNA binding transcription factor (*19*, *20*). RLR activation by dsRNA also induces the NF-κB pathway, which often leads to production of proinflammatory cytokines (*1*, *3*). IRF3 and NF-κB then cooperate to activate IFN-β expression, which initiates an antiviral response by coordinating IRF7- and IRF3-responsive expression of a large number of IFN-stimulated genes (ISGs), to establish an antiviral state for survival in acute viral infection and modulation of the immune response (*1*, *3*).

The activity of MAVS is subjected to posttranslational modifications. K48-linked ubiquitylation, catalyzed by AIP4 or RNF5, leads to MAVS proteasomal degradation (*21*, *22*). Hepatitis C virus NS3/4A protease cleaves MAVS upstream of its transmembrane domain and results in its inactivation (*23*). A very recent report demonstrated that MAVS is the direct substrate of TBK1, which facilitates IRF3 activation (*24*). In contrast to much progress in understanding IRF3 activation, little is known about the molecular basis for maintaining the resting state of MAVS and TBK1/IKKε kinases in the absence of stimulation.

Reversible protein phosphorylation constitutes one of the fundamental regulatory mechanisms governing various biological processes, such as cell growth and differentiation, immune response, metabolism, and neuronal activities. Protein phosphatase magnesium-dependent 1A (PPM1A; also known as PP2Cα) is a member of the PP2C family of Ser/Thr protein phosphatases, a family of phosphatases that are widely expressed across species and are negative regulators of cell stress response pathways (*25*). PPM1A dephosphorylates and inhibits the activation of p38 and c-Jun N-terminal kinase cascades induced by environmental stresses (*26*), and dephosphorylates cyclin-dependent kinases in cell cycle control (*27*). PPM1A also terminates transforming growth factor–β (TGF-β) signaling by dephosphorylating and thereby inactivating

[1]Life Sciences Institute and Innovation Center for Cell Signaling Network, Zhejiang University, Hangzhou 310058, China. [2]Michael E. DeBakey Department of Surgery and Department of Molecular and Cellular Biology, Baylor College of Medicine, Houston, TX 77030, USA. [3]Eye Center of the Second Affiliated Hospital School of Medicine, Institute of Translational Medicine, Zhejiang University, Hangzhou 310058, China.
*These authors contributed equally to this work.
†Corresponding author. Email: xhfeng@zju.edu.cn (X.-H.F.); xupl@zju.edu.cn (P.X.)

Smad2/3, the essential effectors of TGF-β pathway, and by dephosphorylating RanBP3 for efficient nuclear export of Smad2/3 (*28*, *29*). Ppm1a$^{-/-}$ mice show a lasting inflammatory response in wound healing (*30*) and reduced keratinocyte migration upon wounding (*31*). PPM1A was recently reported as a phosphatase of IKKβ (*32*) and RelA (*33*) to terminate NF-κB signaling and as the phosphatase for STING to impede cytosolic DNA sensing in cell cultures (*34*). Further evidence is needed to establish the role of PPM1A in STING-mediated DNA sensing responses and NF-κB signaling in animals.

Here, we revealed that PPM1A associates with both MAVS and TBK1/IKKε kinases, and inhibits their functions by direct dephosphorylation. Forced PPM1A expression attenuates antiviral response against RNA viruses in cells and drives vulnerable phenotype for virus attack in zebrafish. Knockout or knockdown of PPM1A potently enhanced cytosolic RNA sensing and RNA virus defense in cells and in mice. This study therefore illustrates the physiological function of PPM1A in host antiviral defense and provides molecular insights into preventing cytosolic RNA sensing.

RESULTS

PPM1A is identified as a potent suppressor for cytosolic RNA sensing signaling

In an attempt to systemically analyze the effects of reversible phosphorylation for cytosolic RNA sensing, we screened for phosphatases involved in the RLR/IRF3 signaling by using a human phosphatome complementary DNA (cDNA) library (92% coverage) and the IRF3-responsive reporter readout (fig. S1 for Ser/Thr phosphatases). The IFN-β promoter and 5xISRE promoter are highly responsive to the expression of the constitutively active RIG-I (caRIG-I) (Fig. 1A) (*35*) or mitochondria-associated adaptor MAVS (Fig. 1B). PPM1A could profoundly inhibit RIG-I–induced and IRF3-dependent transcription response (Fig. 1A). Similarly, PPM1A completely abolished MAVS or TBK1-stimulated IRF3 activation (Fig. 1B). PPM1A mediated inhibition of IRF3 activation in a dose-dependent manner.

Previous studies reported that Asp^{239} and Arg^{174} residues in the PP2C domain were critical for PPM1A catalytic activity (*28*, *36*). We thereby constructed Asp-to-Asn or Arg-to-Gly substitution at amino acid 239 (D239N) or 174 (R174G) in PPM1A and examined their effects in caRIG-I–stimulated IRF3 responses. As shown in Fig. 1C, D239N mutant exhibited a faster migration as reported by Lin *et al.* (*28*), and both D239N and R174G mutants lost activity to completely block RIG-I–induced IRF3 activation. Activation of cytosolic RNA sensing could also be detected by monitoring the phosphorylation of Ser^{396} at the C terminus of IRF3, which represents IRF3 activation (*37*). Immunoblotting by phosphorylated IRF3 (pIRF3) (S396) antibody revealed a robust IRF3 activation by caRIG-I expression (Fig. 1D). In contrast, coexpression of wild-type PPM1A, but not its D239N or R174G mutant, abolished IRF3 activation (Fig. 1D). Together, both observations illustrate the importance of phosphatase activity for PPM1A to attenuate cytosolic RNA sensing signaling.

Depletion or knockout of PPM1A boosts antiviral responses

To verify the physiological function of PPM1A in cytosolic RNA sensing, we depleted the expression of endogenous PPM1A by small interfering RNA (siRNA) (Fig. 1, E and F, left) or short hairpin RNA (fig. S2, left). Upon PPM1A knockdown, a significantly higher level of IFN-β promoter transactivation could be obtained in response to activated RIG-I [Fig. 1E (middle) and fig. S2 (right)] or by TpIC, a mimetic exposure of cytosolic dsRNA (Fig. 1E, right). We observed an enhanced IRF3 nuclear translocation in PPM1A-depleted cells upon infection of Sendai virus (SeV) (Fig. 1F). Because IFN-β promoter transactivation and nuclear translocation indicate IRF3 activation, we observed stronger phosphorylation on endogenous IRF3 at Ser^{396} residue in response to infection with vesicular stomatitis virus (VSV) (Fig. 1G, left). Consequently, knockdown of PPM1A drastically enhanced the expression of antiviral genes (Fig. 1G, right). These results reveal a negative role of PPM1A on antiviral RLR/IRF3 signaling.

We next isolated and differentiated bone marrow–derived macrophages (BMDMs) from wild-type or Ppm1a$^{-/-}$ mice and evaluated their antiviral responses against SeV infection. As shown in Fig. 1H, an effective induction of mRNA of antiviral genes, such as *IFNB1*, *IFIT1*, *ISG15*, and *IRF7*, was detected upon SeV infection. However, their basal expression and inductions were significantly higher in Ppm1a$^{-/-}$ BMDMs (Fig. 1H and fig. S3). These results further support the repressing function of PPM1A for cytosolic RNA sensing and antiviral responses.

Host defense in Ppm1a$^{-/-}$ cells and mice are enhanced against RNA viruses

To further define the innate antiviral function of PPM1A, we generated Ppm1a$^{-/-}$ 293T cells by CRISPR (clustered regularly interspaced short palindromic repeats)/Cas9 (CRISPR-associated protein 9) genome editing and examined them for antiviral defense by infection of gVSV. As expected, a marked increase of IRF3 activation (Fig. 2A, left) and a drastic decrease of VSV replications were observed in Ppm1a$^{-/-}$ 293T cells, by monitoring GFP protein level (Fig. 2A, left) or virus-replicating GFP^{+} cells (Fig. 2A, right). Likewise, reduced GFP^{+} cell number, that is, VSV-replicating cells, was observed when PPM1A was depleted by siRNA (Fig. 2B). Both results suggest an enhancement of cellular antiviral defense by deletion of PPM1A.

We next challenged wild-type and Ppm1a$^{-/-}$ mice by intravenous injection through the tail vein of gVSV to evaluate the physiological function of PPM1A on antiviral defense by whole animal. As shown in Fig. 2C, a significant reduction of gVSV replications was recorded in Ppm1a$^{-/-}$ mice, on the basis of the quantification of virus loads in livers, spleens, and lungs of sacrificed animals by quantitative real-time polymerase chain reaction (qRT-PCR). These data indicate an enhancement of antiviral defense against gVSV infection in Ppm1a$^{-/-}$ mice. Furthermore, gVSV infection led to the rapid death of wild-type mice at an interval between 10 and 12 hpi, whereas Ppm1a$^{-/-}$ mice exhibited a resistance to gVSV infection with a significantly better survival (Fig. 2D). We also detected an enhanced level of ISGs mRNA in peripheral blood mononuclear cells (PBMCs) from Ppm1a$^{-/-}$ mice at the early stage of gVSV infection (Fig. 2E). Together, these support the notion that PPM1A plays an important physiological function in antiviral defense against RNA virus.

Forced PPM1A expression sensitizes VSV infection on mammalian cells or zebrafish embryos

Expression of MAVS activates antiviral response and endows cells for viral resistance (*16*). As expected, previous expression of MAVS drastically reduced gVSV replication in 293T cells (Fig. 2F, second panel). In contrast, coexpression of wild-type PPM1A, but not its D239N mutants, impaired MAVS-induced viral resistance and restored gVSV replications (Fig. 2F).

We next attempt to investigate PPM1A's function on antiviral defense using an additional animal model. We developed a strategy to rapidly

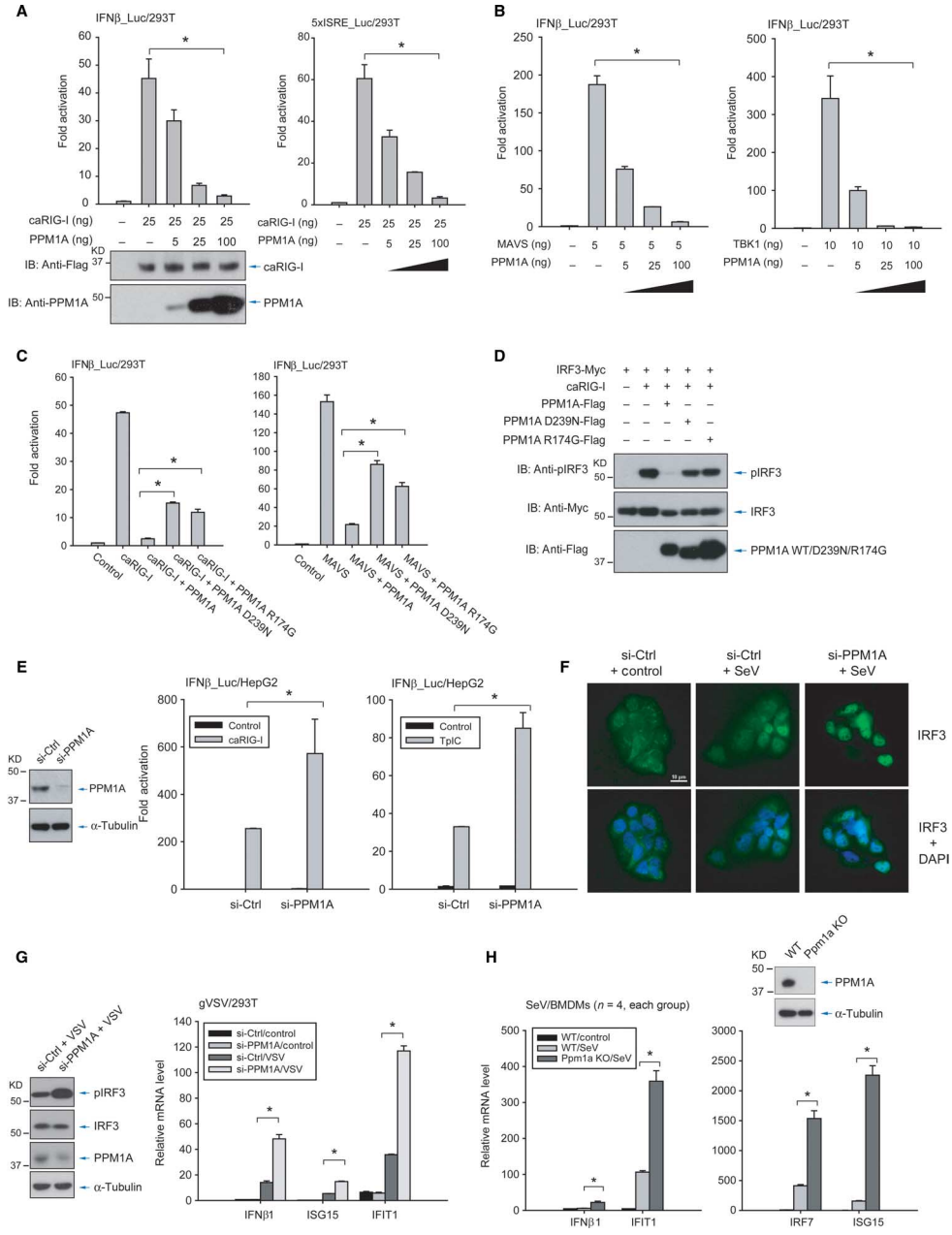

Fig. 1. PPM1A potently suppresses cytosolic RNA sensing and antiviral response. (**A**) In a dose-dependent manner, transfection of PPM1A elicited a marked suppression on IRF3-responsive IFN-β promoter (left) or 5xISRE promoter (right) in 293T cells, which was stimulated by expression of activated RIG-I (caRIG-I). The comparative level of PPM1A and caRIG-I was detected by immunoblotting (IB) (left). $n = 4$ experiments. *$P < 0.001$, compared with control, by Student's t test. (**B**) PPM1A also strongly inhibited IRF3 activation, which was stimulated by either adaptor MAVS (left) or kinase TBK1 (right), in a dose-dependent manner. $n = 3$ experiments. *$P < 0.001$, compared with control, by Student's t test. (**C**) Transfection of PPM1A D239N or R174G mutant that is catalytically defective, but not PPM1A wild type (WT), has a much weaker effect on caRIG-I–stimulated IRF3 activation. $n = 3$ experiments. *$P < 0.001$, compared with WT PPM1A, by Student's t test. (**D**) caRIG-I–induced IRF3 activation, as revealed by anti-pIRF3 (Ser^{396}) immunoblotting (top), was completely abolished by cotransfection of PPM1A WT, but not its phosphatase-defective forms. (**E**) Transfection of siRNA-targeting PPM1A (si-PPM1A) in HepG2 cells, which effectively depleted endogenous PPM1A expression (left), enhanced cytosolic RNA sensing in response to either caRIG-I stimulation or polyinosinic-polycytidylic acid [poly(I:C)] transfection (TpIC) (middle and right). $n = 3$ experiments. *$P < 0.01$, compared with control siRNA (si-Ctrl), by Student's t test. (**F**) siRNA-mediated PPM1A depletion promoted SeV-induced nuclear translocation of endogenous IRF3, which was detected by immunofluorescence and microscopy. DAPI, 4′,6-diamidino-2-phenylindole. (**G**) Similar siRNA-mediated depletion of PPM1A in 293T cells, as displayed by immunoblotting of PPM1A (left), boosted VSV-induced IRF3 Ser^{396} phosphorylation (left) and enhanced antiviral response measured by virus-induced mRNA expression of antiviral proteins, including IFNB1, ISG15, and IFIT1 (right). gVSV, green fluorescent protein (GFP)–tagged VSV. (**H**) Antiviral response of control or $Ppm1a^{-/-}$ BMDMs against SeV infection was measured by mRNA induction at 12 hours post-infection (hpi) of various ISGs. $Ppm1a^{-/-}$ BMDMs exhibited stronger antiviral responses compared to control BMDMs. PPM1A expression was revealed by anti-PPM1A immunoblotting. $n = 4$ mice. *$P < 0.01$, compared with control, by Student's t test. KO, knockout.

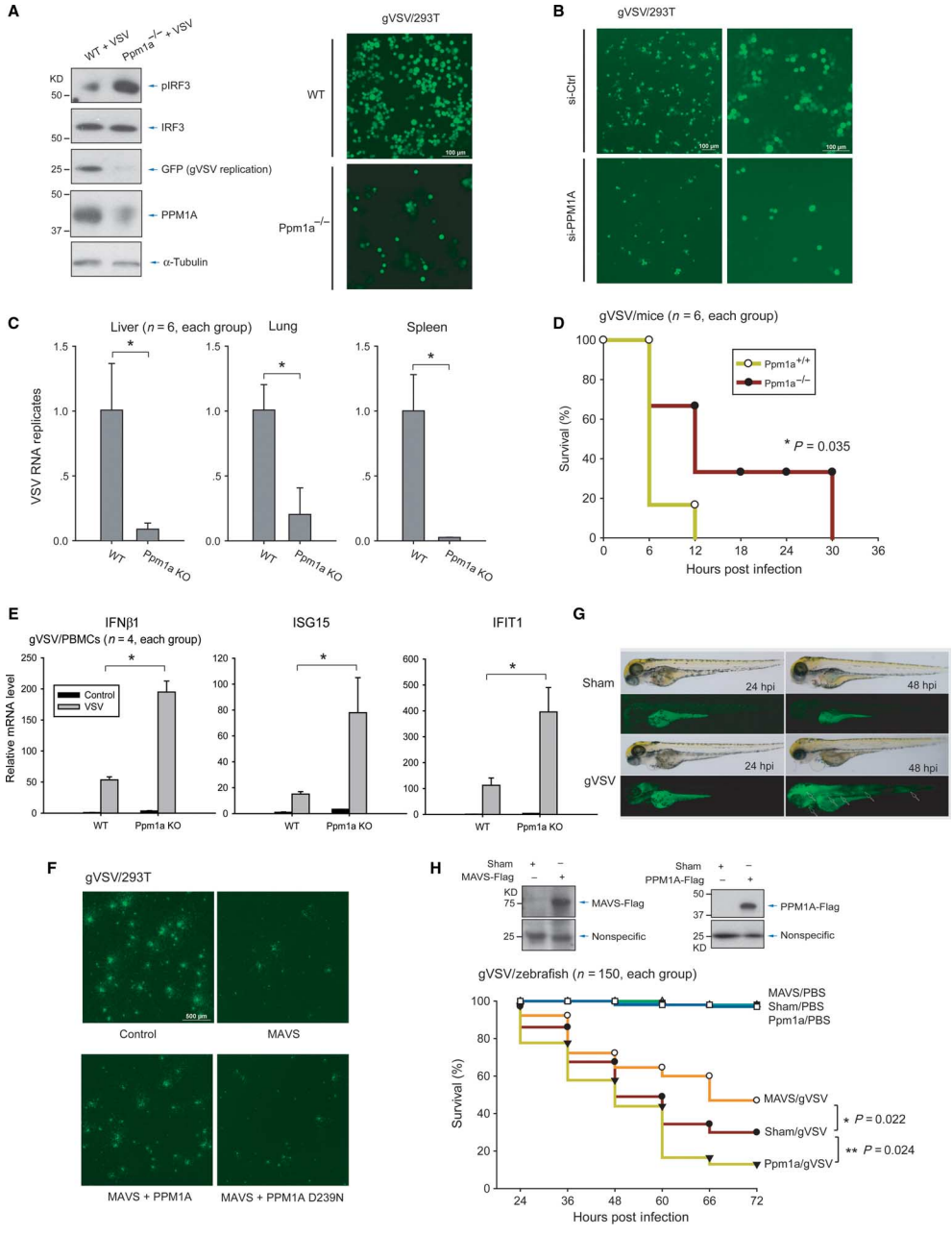

Fig. 2. PPM1A negatively regulates host antiviral defense in cells, mice, and zebrafish. (**A**) Ppm1a$^{-/-}$ 293T cells were generated by CRISPR/Cas9 strategy and infected with gVSV. An enhanced IRF3 activation induced by gVSV infection was detected by phospho-Ser^{396} immunoblotting when PPM1A was knocked out. Drastically boosted cellular viral resistance was observed by less amount of total GFP tags detected by immunoblotting (left) or by reduced virus-replicating (GFP^{+}) cells (right). (**B**) siRNA-mediated depletion of PPM1A in 293T cells, as indicated in Fig. 1G, led to effectively reduced infection of gVSV. (**C**) Determination of gVSV loads in mouse organs by $TCID_{50}$ (median tissue culture infectious dose) assay 12 hpi in Ppm1a$^{-/-}$ and WT mice, which were intravenously injected through the tail vein with gVSV. $n = 6$ mice for each group. *$P < 0.01$, compared with control Ppm1a$^{+/+}$ group, by Student's t test. (**D**) Survival of ~8-week-old Ppm1a$^{-/-}$ and WT mice given intravenous tail vein injection of gVSV [2×10^7 plaque-forming units (PFU)/g]. $n = 6$ mice for each group. $P < 0.05$, by paired Student's t test. (**E**) Enhanced antiviral response was detected in Ppm1a$^{-/-}$ PBMCs by mRNA induction of antiviral proteins, including IFNB1, ISG15, and IFIT1 at 6 hpi of VSV injection in mice. $n = 4$ mice for each group. *$P < 0.05$, compared with control Ppm1a$^{+/+}$ group, by Student's t test. (**F**) 293T cells, which were previously transfected with MAVS in the absence or presence of PPM1A WT or phosphatase-defective mutant, were infected by gVSV. Visualized GFP represented cells that have active VSV replication. Restored numbers of virus-replicating (GFP^{+}) cells indicated that overexpression of PPM1A impeded antiviral function of MAVS. (**G**) gVSV was microinjected into yolk of zebrafish embryos (1×10^3 PFU per embryo), which elicited a robust virus infection status and occurred strongly at brain but was also visible at muscle and gut tissues of fish. The infection was aggravated at 48 hpi and started to cause embryo death. (**H**) Zebrafish embryos were previously microinjected with MAVS or PPM1A mRNA to gain expression of proteins, as detected by immunoblotting (top). The survival rates of gVSV-infected zebrafish were recorded. A vulnerable phenotype of PPM1A- expressing embryos and a resistance phenotype of MAVS-expressing embryos to gVSV infection were observed upon VSV challenge. $n = 150$ embryos for each group. *$P < 0.05$, **$P < 0.05$, compared with sham group, by paired Student's t test. PBS, phosphate-buffered saline.

assess the antiviral regulation in zebrafish, by combining genetic manipulation and microinjection of gVSV for infection at the early stage of zebrafish embryogenesis. Microinjection of in vitro–transcribed mRNA resulted in forced expression of exogenous human MAVS or PPM1A, and embryos with normal development were selected for the gVSV virus injection at embryo yolk at 48 hours post-fertilization (hpf). As shown in Fig. 2G, zebrafish embryos underwent a clear VSV infection upon gVSV injection in yolk, mainly at brain tissue, but VSV replications at muscle and gut tissues were also found. The infection was at a relatively weak level at 24 hpi but exaggerated at 48 hpi, which could cause embryo death. As a positive control, human MAVS expression promoted the tolerance of embryos to VSV infection, as shown by significantly reduced embryo lethality (Fig. 2H), confirming its function on host defense in zebrafish. However, human PPM1A (hPPM1A) expression significantly decreased the tolerance of embryos to VSV infection (Fig. 2H), in agreement with its potential in suppressing antiviral defense. It also illustrates that PPM1A antiviral function is evolutionarily conserved.

PPM1A is an inherent component and silencer of TBK1/IKKε complex

Given the importance of PPM1A on antiviral physiology, we attempted to dissect the molecular basis for PPM1A-mediated function. In coimmunoprecipitation, by using either anti-TBK1 or anti-IKKε antibody, we detected a strong signal of endogenous PPM1A that associated with endogenous TBK1/IKKε, demonstrating that PPM1A is one of the components of TBK1/IKKε complex (Fig. 3, A and B). A robust signal of endogenous PPM1A was revealed by mass spectrometry analysis of TBK1-interacting proteins from 293T cell lysates (Fig. 3C). Using immunofluorescence combined with super-resolution microscopy, we also observed an image of colocalization of endogenous PPM1A with TBK1 and its distinct distribution in response to TBK1 ectopic expression (fig. S4). These consistent observations strongly indicate that PPM1A is an inherent component of TBK1/IKKε complex. Subsequently, domain mapping analysis for the interaction between full-length PPM1A and TBK1 truncations (Fig. 3D, left) revealed that the kinase domain of TBK1 was capable of and sufficient in recruiting PPM1A (Fig. 3D, right).

On the basis of these observations, we analyzed the effects of PPM1A on TBK1/IKKε complex. We found that PPM1A abolished the C-terminal phosphorylation of IRF3 (Fig. 1D), whereas depletion of PPM1A expression improved virus-induced pIRF3 level (Figs. 1G and 2A). These observations suggest that PPM1A may block kinase activities of TBK1/IKKε. We then performed an in vitro kinase assay using separately purified IRF3 and TBK1; the latter was cotransfected with or without PPM1A, wild type or phosphatase-defective (Fig. 3E, left). As expected, IRF3 was robustly phosphorylated by separately purified TBK1 (Fig. 3E, right). However, a complete loss of TBK1 kinase activity was observed when TBK1 was cotransfected with wild-type PPM1A, indicating that PPM1A dampened the catalytic activity of TBK1 (Fig. 3E, right). In contrast, stronger TBK1 activation upon stimulation by either RIG-I or STING, measured by Ser^{172} phosphorylation, was detected when PPM1A was depleted by siRNA (Fig. 3F). These observations collectively demonstrate that PPM1A interacts with, and abolishes the activation of, TBK1/IKKε and eliminates their catalytic activities.

PPM1A directly dephosphorylates both MAVS and TBK1/IKKε

MAVS was phosphorylated by TBK1, and this "reverse-directed" phosphorylation is critical for the formation of active signal complex to drive IRF3 activation (*24*). We thus evaluated the effect of PPM1A on MAVS phosphorylation. By using in vitro phosphatase assays, purified PPM1A was incubated with isolated MAVS that was cotransfected with TBK1 in cells and, thus, phosphorylated by TBK1 (Fig. 4A, left). As expected, cotransfection of TBK1 led to massive phosphorylation on MAVS, as evidenced by strong MAVS mobility shift on electrophoresis (Fig. 4A, second lane of right panel). Similar to λ protein phosphatase (λPPase), purified PPM1A completely eliminated phosphorylation on MAVS, indicating that PPM1A directly dephosphorylated phospho-MAVS (Fig. 4A). In contrast, catalytically defective PPM1A did not remove MAVS phosphorylation. Cotransfection of PPM1A also eliminated MAVS phosphorylation in cells (Fig. 4B, third lane). Although interaction between MAVS and PPM1A was weak, it was substantially enhanced in the presence of IKKε (Fig. 4C), suggesting that TBK1/IKKε recruited PPM1A to MAVS for subsequent dephosphorylation. Using coimmunoprecipitation assay, we detected association of endogenous PPM1A with endogenous MAVS upon VSV infection (Fig. 4D), and using immunofluorescence, we observed obvious recruitment of endogenous PPM1A to mitochondria upon SeV infection (Fig. 4E). All observations thus suggest a virus-induced formation of PPM1A and MAVS complex.

In a similar in vitro phosphatase assay, incubation of PPM1A also eliminated TBK1/IKKε phosphorylation at Ser^{172} residue, evidenced by phospho-S172 immunoblotting (Fig. 4, F and G). When compared with PPM1B, PPM1A-mediated TBK1/IKKε dephosphorylation was robust, similar to the action of λPPase (Fig. 4H), and resulted in a complete inactivation of TBK1/IKKε (Fig. 4, F to H). Hereby, it suggests a dual mechanism for PPM1A action on cytosolic RNA sensing signaling, that is, directly dephosphorylating both adaptor MAVS and kinases TBK1 and IKKε.

Balance between PPM1A and MAVS determines antiviral signal output

MAVS colocalizes with the TBK1/IKKε kinase complex and IRF3 to transduce signal (*24*). As expected, the formation of signaling complex of cytosolic RNA sensing, that is, association of MAVS/IKKε, was detected by coimmunoprecipitation (Fig. 5A). The presence of wild-type, but not phosphatase-defective, PPM1A effectively disrupted both the MAVS/IKKε and MAVS/TBK1 complexes (Fig. 5, A and B), demonstrating that dephosphorylation of MAVS and kinases can substantially damage the signal complex. In contrast, a stronger signal of TBK1/IRF3 interaction was observed when endogenous PPM1A was depleted by siRNA interference, thus illustrating the negative regulation of PPM1A on TBK1/IRF3 complex formation (Fig. 5C). Note that an IRF3 2SA mutant was used in the coimmunoprecipitation assay to enhance its association with kinase TBK1 (*24*). Association of PPM1A/IKKε was largely eliminated when a high level of MAVS was forcedly expressed (Fig. 5D), indicating that the balance between MAVS and PPM1A may dictate the signal output for cytosolic RNA sensing. Unexpectedly, although PPM1A disrupted the complex of TBK1/IKKε kinases with adaptor MAVS or with substrate IRF3, it actually enhanced the association between MAVS and IRF3 (Fig. 5E), a possible trapping of both proteins in the complex without active kinases.

Therefore, we propose a working model for PPM1A's mechanism in modulating cytosolic RNA sensing signaling, in which PPM1A is an integral component, recruited by TBK1/IKKε to dephosphorylate and antagonize functions of both MAVS and TBK1/IKKε. In accordance, PPM1A acts as a silencer and disrupts the signal output for IRF3 activation. Through this, PPM1A physiologically controls host antiviral defense

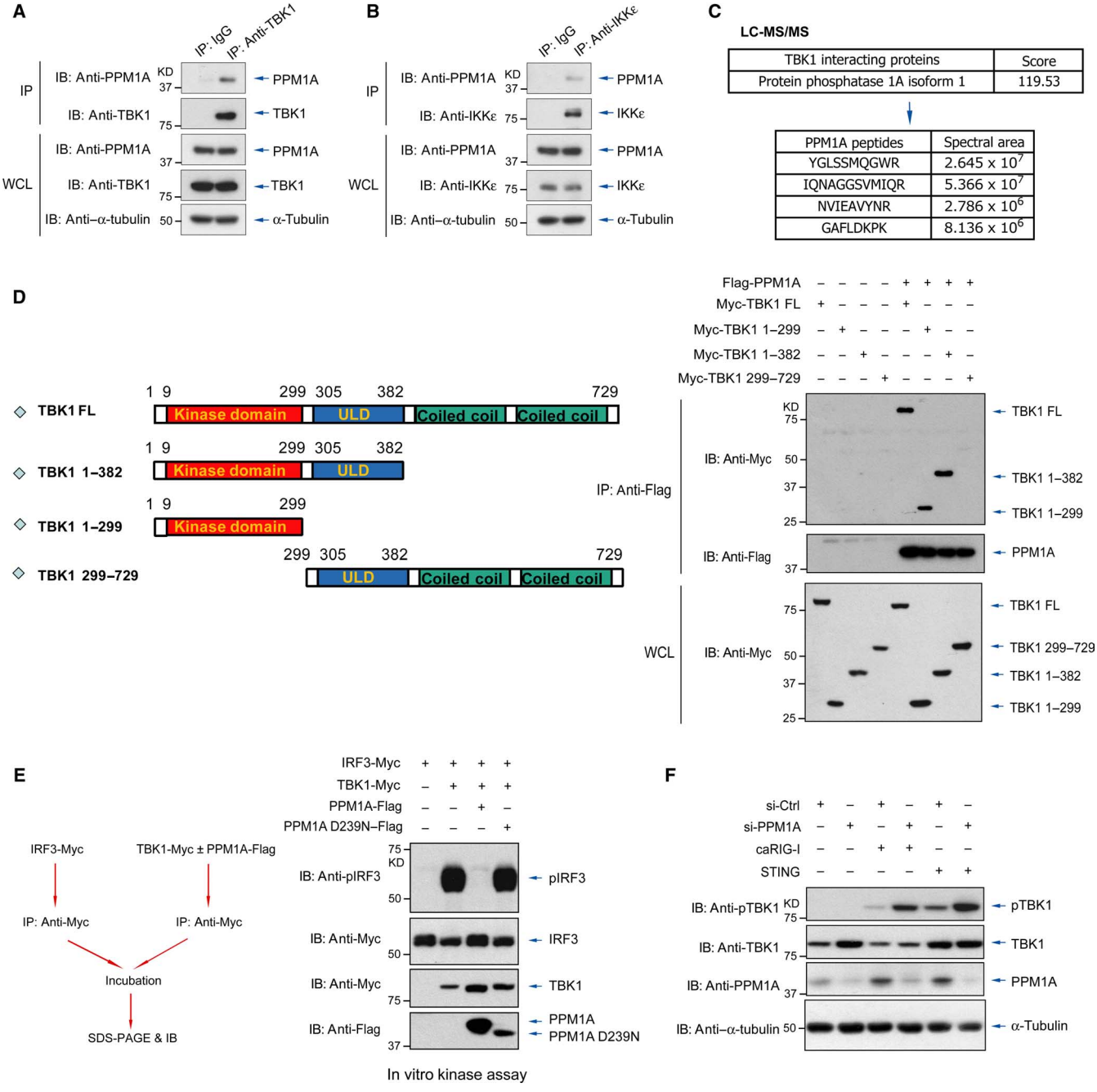

Fig. 3. PPM1A is an inherent component and silencer of TBK1/IKKε complex. (**A** and **B**) Endogenous complex of PPM1A/TBK1 or PPM1A/IKKε was detected by coimmunoprecipitation using anti-TBK1 or anti-IKKε antibodies in 293T lysates and visualized by anti-PPM1A antibody. IgG, immunoglobulin G; IP, immunoprecipitation; WCL, whole-cell lysates. (**C**) Peptides of endogenous PPM1A were detected in abundance by mass spectrometry in TBK1-immunoprecipitated proteins by Flag tag, verifying that PPM1A was an endogenous component of TBK1 complex. LC-MS/MS, liquid chromatography–tandem mass spectrometry. (**D**) Domain mapping assays, performed by coimmunoprecipitation of Flag-tagged full-length (FL) PPM1A with serial truncations of TBK1 (left), revealed that the C terminus, that is, kinase domain of TBK1, was responsible and enough to recruit PPM1A (right). ULD, ubiquitin-like domain. (**E**) In vitro kinase assay was performed using separately purified IRF3 and TBK1, which was cotransfected with or without PPM1A (left), showing that TBK1 coexpressed with WT PPM1A lost its kinase ability to phosphorylate IRF3. SDS-PAGE, SDS–polyacrylamide gel electrophoresis. (**F**) siRNA-mediated depletion of PPM1A in 293T cells resulted in an enhanced activation of endogenous TBK1, in response to stimulations from activated RIG-I or STING. pTBK1, phosphorylated TBK1.

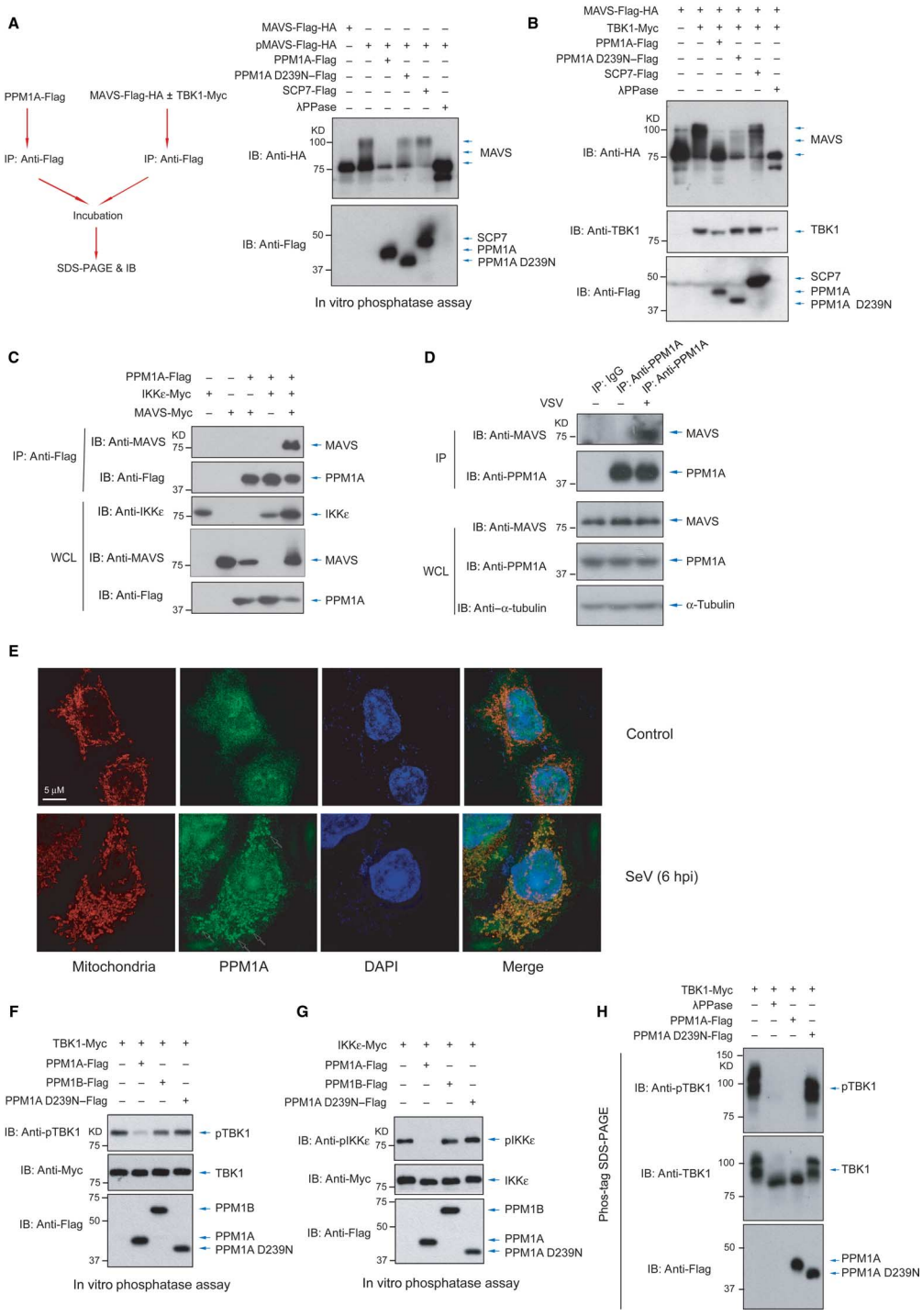

Fig. 4. PPM1A directly dephosphorylates MAVS and TBK1/IKKε. (**A**) In vitro phosphatase assays were performed by using purified PPM1A and separately isolated MAVS, which were previously coexpressed with TBK1 to gain phosphorylation modifications, as visualized by mobility shift (second lane). WT PPM1A, but not phosphatase SCP7 that was set as a negative control, removed phosphorylation on MAVS, similar to λPPase treatment. HA, hemagglutinin. (**B**) Similarly, coexpression of PPM1A with both MAVS and TBK1 in 293T cells led to disappearance of phospho-MAVS modifications, as monitored by mobility shift. (**C**) Coimmunoprecipitation with tagged MAVS and PPM1A showed that only minimal interaction between PPM1A and MAVS was detected, but their interaction was drastically enhanced in the presence of IKKε. (**D**) Endogenous complex of PPM1A/MAVS was detected upon VSV infection at 6 hpi by coimmunoprecipitation using anti-PPM1A antibody in 293T lysates and visualized by anti-MAVS antibody. (**E**) A significant portion of endogenous PPM1A (by anti-PPM1A antibody; green) was translocated to mitochondria (by MitoTracker staining; red) upon SeV infection at 6 hpi, captured, and visualized by immunofluorescence and the super-resolution microscopy. (**F** and **G**) In vitro phosphatase assays were performed by using separately purified TBK1 or IKKε with PPM1A WT or its phosphatase-defective mutant, showing that WT PPM1A eliminated phospho-Ser^{172} modification on TBK1 (F) or IKKε (G). (**H**) Phos-tag SDS-PAGE showed that PPM1A removed phosphorylation modifications on TBK1 to an extent similar to λPPase treatment (second panel).

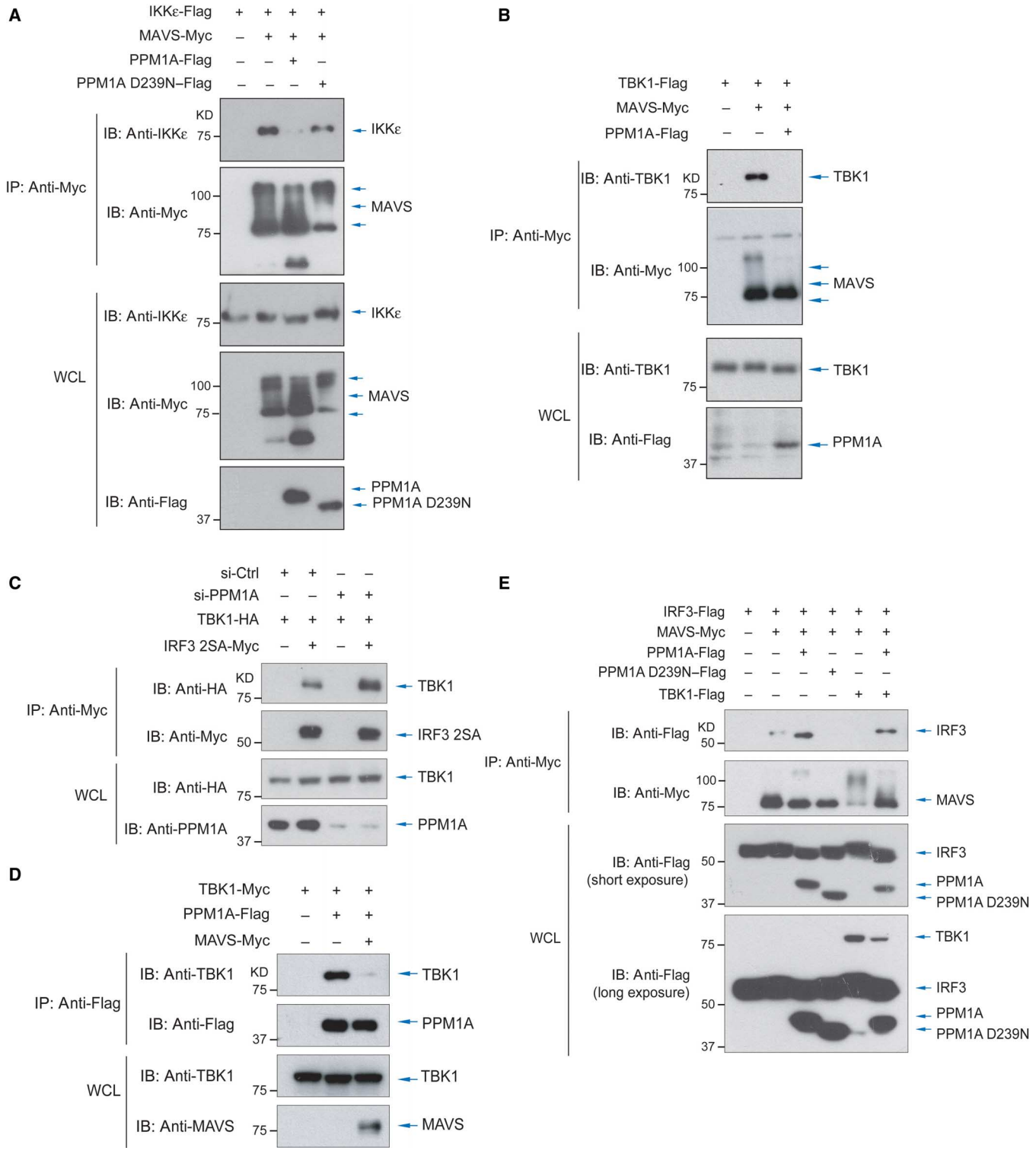

Fig. 5. PPM1A and MAVS compete for antiviral signaling output. (**A**) Coimmunoprecipitation assay revealed that MAVS/IKKε association was disrupted in the presence of WT PPM1A, but not by its phosphatase-defective form. Note the faster mobility shift of IKKε and MAVS in the presence of WT PPM1A (third panel), indicating the dephosphorylation of both kinase and adaptor by PPM1A in cells. (**B**) Similarly, interaction between MAVS and TBK1 was diminished by WT PPM1A. (**C**) Interaction of TBK1 with IRF3 2SA mutant, which had an enhanced interaction to TBK1 and thereby used in analysis for TBK1/IRF3 interaction, was significantly improved by the siRNA-mediated depletion of PPM1A expression. (**D**) Coimmunoprecipitation assay with Myc-tagged TBK1 and Flag-tagged PPM1A revealed their strong association. The presence of cotransfected MAVS can lower TBK1 and PPM1A interaction. (**E**) Coimmunoprecipitation assay of Flag-tagged IRF3 with Myc-tagged MAVS, with or without PPM1A, showed that PPM1A enhanced IRF3/MAVS association, possibly by trapping IRF3 in an inactive MAVS.

against RNA viruses in cells and on whole animals from fish to mammals (Fig. 6).

DISCUSSION

Pathogenic nucleic acid is sensed in cytoplasm by RLRs and other molecules including cGAS, DDX16, DAI, and RNA polymerase III, which activate the antiviral response to danger signals through adaptor MAVS or STING (*38*, *39*). Extensive studies have illustrated that the innate antiviral signaling is modulated by a variety of intracellular molecules, including (de)ubiquitylases, kinases, and phosphatases (*40*). Here, we show that phosphatase PPM1A is an endogenous component of the TBK1/IKKε complex and governs antiviral defense through a dual action to eliminate phosphorylation on both MAVS and TBK1/IKKε. PPM1A eliminates TBK1-induced phosphorylation on MAVS, which is reported to be essential for the integrity of MAVS complex (*24*), and removes Ser^{172} phosphorylation on both TBK1 and IKKε, which is indispensible for their signal-induced activation. In accordance, PPM1A blocks cytosolic RNA sensing signaling and weakens RNA virus resistance on two distinct animal species. Therefore, the inherent level and activity of a phosphatase can integrate and coordinate the innate defense and dictate the outcome of host antiviral resistance of host cells and animals.

The finding that PPM1A controls threshold of cells for sensing danger signal, such as heterogeneous RNA, adds new dimensions for PPM1A function. It could be an adaptive mechanism to ensure the removal of pathogenic factors; however, it adds another layer of protection to avoid autoimmune damages by hypersensitive responses to leaking signal, such as from the exposure of self-RNAs in cytosol. Therefore, the direct inhibition of cytosolic RNA sensing by PPM1A provides a mechanism to ensure cell survival when favorable conditions are available. Currently, much less is known about how PPM1A activity and level are regulated by intracellular conditions or extracellular cues (fig. S5). Inhibition of MAVS and TBK1/IKKε function by PPM1A may also contribute to the apoptosis regulation and the tumor-suppressing activity of TBK1; however, this hypothesis needs further validations.

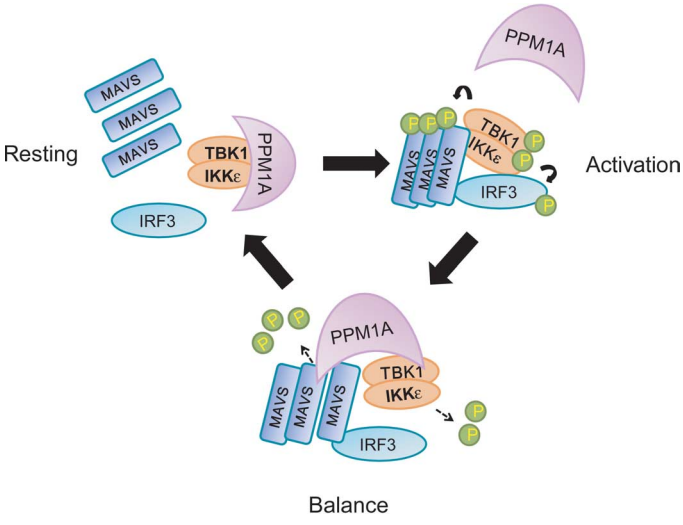

Fig. 6. Model for PPM1A-guided silencing of cytosolic RNA sensing and antiviral defense. Phosphatase PPM1A is a natural component of TBK1/IKKε kinase complex, which is recruited by kinase domains of TBK1/IKKε to restrain cytosolic RNA sensing by directly dephosphorylating both MAVS and TBK1/IKKε, potentially serving as a threshold check of antiviral signaling. However, stronger activation from MAVS can release TBK1/IKKε from the grasp of PPM1A, leading to their activation and MAVS phosphorylation which led to IRF3 C-terminal phosphorylation and translocation to function as transcriptional factor.

Mechanism for PPM1A-mediated silence of cytosolic RNA sensing

MAVS is central for cytosolic RNA sensing and host defense against RNA viruses. By acting downstream of RIG-I and MDA5, MAVS links and coordinates pathways to the activation of both TBK1/IKKε and NF-κB, leading to the subsequent induction of antiviral cytokines, such as type I and type III IFNs (*3*, *41*). Once activated by RIG-I/MDA5, MAVS self-associates and polymerizes to form 400-nm-long and three-stranded helical filaments on mitochondria (*18*), which involves a complicated interactome including ubiquitin E3 ligases (TRAF2, TRAF6, and ITCH), deubiquitylase CYLD, kinases [IKKε, CHUK (conserved helix-loop-helix ubiquitous kinase), RIPK1 (receptor-interacting protein kinase 1)], adaptor protein FADD (Fas-associated death domain protein), and signal mediator IRF3 (*18*, *42*–*45*). Recently, Liu *et al.* (*24*) illustrated that TBK1 directly modifies MAVS on multiple sites, and phosphorylation at Ser^{464} cluster enhances the formation of MAVS complex and IRF3 activation.

Our current results show that PPM1A is an endogenous partner of IKKε/TBK1 and is recruited to MAVS to regulate MAVS function by eliminating phosphorylation on MAVS. Inhibition of MAVS function by PPM1A involves a dual mechanism, that is, inhibition of TBK1-mediated MAVS phosphorylation and dephosphorylation of Ser^{172} residue on both TBK1/IKKε themselves. An interesting observation is that PPM1A is an inherent partner of TBK1/IKKε yet weakly associated with MAVS. IKKε bridges the strong interaction between MAVS and PPM1A. Through this interaction, PPM1A can remove all phosphorylation on MAVS. Thus, we identified PPM1A as the first phosphatase of MAVS, the key adaptor for cytosolic RNA sensing. TBK1-mediated MAVS phosphorylation was thought to favor IRF3 recruitment on MAVS (*24*). Thus, PPM1A-mediated MAVS dephosphorylation compromises IRF3 activation. It is possible that PPM1A might have effects on MAVS phosphorylation by kinases other than TBK1.

Furthermore, PPM1A, but not PPM1B, serves as an efficient phosphatase to dephosphorylate Ser^{172} residue of both TBK1 and IKKε kinases, which is critical for their kinase activities (*46*). PPM1B is previously reported to dephosphorylate TBK1 and inhibit its activation, although no physiological function is presented (*47*). Collectively, PPM1A-mediated removal of TBK1-induced MAVS phosphorylation and the elimination of TBK1/IKKε activation lead to a profound inhibitory effect on cytosolic RNA sensing and, at the same time, a drastic phenotype at the cellular or animal level for viral resistance when PPM1A expression is either enforced or silenced.

Physiologies of PPM1A in viral pathogen sensing and host defense

A few phosphatases have been documented to engage in antiviral host defense, such as SHP-1 (Src homology region 2 domain-containing phosphatase-1) (*48*), PP1 (protein phosphatase 1) (*49*, *50*), PP4 (*51*), PPM1B (*52*), PP2A (*53*), and DUSP1 (dual specificity phosphatase 1) (*54*). Most of the phosphatases target cytosolic RNA sensors, including RIG-I and MDA5 or effector IRF3. While our manuscript was in preparation, a recent study reported that PPM1A serves as the phosphatase

of STING, which would regulate its aggregation and activation (*34*). However, in vivo evidence for PPM1A in cytosolic DNA sensing remains lacking. Our current study identifies PPM1A as the first MAVS phosphatase and shows PPM1A as a physiological regulator of RNA virus resistance across species, from zebrafish to mammals.

On the other hand, repression of cytosolic RNA sensing and IRF3 responsiveness by PPM1A may substantially affect many processes that are controlled by host defense. MAVS, TBK1 and/or IKKε, and IRF3 are widely expressed, and IRF3 can be activated by DNA damage, membrane fusion, and endoplasmic reticulum stress, in addition to virus infection. In accordance, the expression level, activity, and subcellular compartments of PPM1A, which are less known, could be important factors for determining the physiologies of MAVS and TBK1/IKKε, as well as hundreds of IRF3-induced ISGs, directly or indirectly. In addition, we have seen a moderate increase of IRF3 responsiveness by ISG production in Ppm1a$^{-/-}$ BMDMs or PBMCs without viral stimulation (Fig. 2E and fig. S3), suggesting a possible basal derepression of IRF3 signaling with PPM1A ablation. A recent report showed that the absence of PPM1A led to enhanced and lasting inflammatory response (*30*), setting it as an effector on wound healing–inflammation–angiogenesis axis in mice. Although different from severe and fatal inflammatory response in Socs1$^{-/-}$ mice (*55*), Ppm1a$^{-/-}$ mice mostly display a normal phenotype, which suggests a milder effect of a basal derepression of IRF3. Cytosolic RNA sensing is normally not agitated by endogenous host RNA, because these sensors (RIG-I/MDA5/LGP2) strictly require pathogen pattern to recognize dsRNA with certain length and 5′-triphosphate, which is absent in endogenous RNA. There are also a few layers of checkpoint to avoid unexpected activation of this danger signal, such as various ubiquitylation or phosphorylation on RIG-I/MDA5 receptors, MAVS adaptor, and TBK1 (*2*). In accordance, deficiency of only one TBK1/MAVS inhibitor might not be sufficient to drive TBK1 activation, although it can enhance the viral-induced TBK1 activation. It is interesting to investigate whether enhanced host defense mechanism is involved in observed up-regulation of inflammation in Ppm1a$^{-/-}$ mice.

In conclusion, our study provides a novel physiological function and mechanistic insights for signal integration of phosphatase PPM1A in cytosolic RNA sensing regulation. Our model indicates that the level and activity of PPM1A can be a determining factor for host defense against RNA viruses, at the level of cells and whole animals. Consistent with this notion, our study proposes that pharmacological suppression of PPM1A, such as by membrane-permeable molecules, may offer a potential therapeutic benefit for antiviral prevention.

MATERIALS AND METHODS

Expression plasmids, reagents, antibodies, and mice

Expression plasmids encoding Flag-, Myc-, or HA-tagged human TBK1, IKKε, IRF3, caRIG-I, MAVS, STING, PPM1A or its D239N and R174G mutations, and the IRF3/7-responsive reporters IFNβ_Luc and 5xISRE_Luc have been described by Lin *et al.* (*28*) and Xu *et al.* (*56*). Site-directed mutagenesis was used to generate expression plasmids encoding TBK1/IKKε with amino acids Ser^{172} replaced by Ala or Glu. TBK1 truncations, including TBK1 amino acids 1 to 299, 1 to 382, and 299 to 729 were generated by PCR-based cloning, which was performed using a kit from Stratagene. Detailed information will be provided upon request. All coding sequences were verified by DNA sequencing.

Poly(I:C) was from Invivogen. GFP- and luciferase-tagged herpes simplex virus–1 (HSV-1) was a gift from J. Han (Xiamen University, Xiamen). gVSV was a gift from Z. J. Chen (University of Texas Southwestern Medical Center, Dallas). SeV (Cantell strain) was from Charles River Laboratories. λPPase was from BioLabs. The monoclonal anti-IRF3, anti-pIRF3, anti-TBK1, anti-pTBK1 (S172), anti-IKKε, anti-IKKε (S172), anti-MAVS, anti-Myc, anti-PPM1A, and anti-HA antibodies were from Cell Signaling Technology. Anti–α-tubulin and anti-Flag antibodies were from Sigma. Ppm1a$^{-/-}$ C57BL/6 mice were generated by Feng Laboratories.

Cell culture, transfections, and infections

Mouse embryonic fibroblasts and human embryonic kidney (HEK) 293, HepG2, HeLa, and HaCaT cells were cultured in Dulbecco's modified Eagle's medium with 10% fetal bovine serum. Primary wild-type or Ppm1a$^{-/-}$ mouse BMDMs were isolated, expanded, and cultured conventionally. X-tremeGENE HP (Roche) or polyethylenimine (PEI; Polysciences) transfection reagents were used for transfection. Infection of SeV and VSV was as described by Xu *et al.* (*56*).

Luciferase reporter assay

Cells were transfected with IRF3/7-responsive IFNβ_Luc or 5xISRE_Luc reporter bearing an open reading frame coding firefly luciferase, along with the pRL-Luc, with *Renilla* luciferase coding as the internal control for transfection, and other expression vectors as specified in Results. After 24 hours of transfection and with the indicated treatment, cells were lysed by passive lysis buffer (Promega). Luciferase assays were performed using a Dual-Luciferase Assay kit (Promega), quantified with POLARstar Omega (BMG Labtech), and normalized to the internal *Renilla* luciferase control.

Quantitative RT-PCR assay

Cells were lysed, and total RNA was extracted using RNeasy extraction kit (Invitrogen). cDNA was generated by one-step iScript cDNA Synthesis Kit (Bio-Rad), and qRT-PCR was performed using the EvaGreen qPCR MasterMix (abm) and CFX96 Real-Time PCR System (Bio-Rad). Relative quantification was expressed as $2^{-\Delta Ct}$, where C_t is the difference between the main C_t value of triplicate of the sample and that of an endogenous L19 or GAPDH (glyceraldehyde-3-phosphate dehydrogenase) mRNA control. The human and mouse primer sequences used are listed in the Supplementary Materials.

Coimmunoprecipitations and immunoblottings

HepG2 or 293T cells were infected with VSV or transfected with plasmids encoding N-terminal Myc-, Flag-, or HA-tagged PPM1A, TBK1, IKKε, IRF3, caRIG-I, MAVS, or STING, as indicated, and lysed using MLB buffer (*57*). Lysates were subjected to immunoprecipitation using anti-Flag (Sigma) or anti-HA (Cell Signaling Technology) antibodies for transfected proteins, or anti-IRF3, anti-TBK1, anti-IKKε, anti-MAVS, or anti-PPM1A antibodies for endogenous proteins. After three to four washes with MLB, adsorbed proteins were analyzed by SDS-PAGE (Bio-Rad) and immunoblotting with the indicated antibodies. Cell lysates were also analyzed by SDS-PAGE and immunoblotting to control protein abundance.

RNA interference

To silence endogenous PPM1A expression in 293T or HepG2 cells, double-stranded siRNA (RiboBio) targeted the hPPM1A mRNA sequence 5′-GUACCUGGAAUGCAGAGUA-3′ (SIB1252115834). Cells were transfected with siRNA using Lipofectamine RNAiMAX (Invitrogen)

for 48 hours before further assay. The reverse transfection method was used to reach optimal efficiency.

In vitro phosphatase or kinase assay

293T cells were transfected with Myc-TBK1, HF-MAVS, or Flag-PPM1A plasmid with the indicated proteins. Immunoprecipitations were performed using anti-Myc or anti-Flag antibody, after 36 hours of transfection. With four washes, immunoprecipitated Myc-TBK1 or HF-MAVS and Flag-PPM1A were incubated in phosphatase assay buffer [20 mM tris-HCl, 1 mM EGTA, 5 mM $MgCl_2$, 0.02% 2-mercaptoethanol, 0.03% Brij-35, BSA (0.2 mg/ml)] at 25°C for 60 min for the phosphatase assay. Kinase assay was performed in the same buffer with addition of 20 μM adenosine 5′-triphosphate, at 30°C for 60 min. Reaction was stopped by addition of 2×SDS loading buffer.

Immunofluorescence and microscopy

To visualize the subcellular localization of TBK1, IRF3, and PPM1A, HaCaT or HeLa cells were treated as indicated in the figures, fixed in paraformaldehyde, permeabilized, and blocked by horse serum. Cell sides were then incubated sequentially with primary antibodies (anti-IRF3, anti-PPM1A, or anti-Myc) and Alexa-labeled secondary antibodies, followed by extensive washing. Slides were then mounted with VECTASHIELD and stained with DAPI (Vector Laboratories). Mitochondria were visualized by MitoSox Red (Life). Immunofluorescence images were obtained and analyzed using a Nikon Eclipse Ti inverted microscope, or GE DeltaVision OMX system, and ImageJ software.

Nano–LC-MS/MS analysis

Nano–LC-MS/MS analysis for protein identification and label-free quantification was performed by PHOENIX national proteomics core service as described by Ding *et al.* (*58*). Tryptic peptides were separated on a C18 column and analyzed by LTQ-Orbitrap Velos (Thermo). Proteins were identified using National Center for Biotechnology Information of human or mouse RefSeq protein databases.

CRISPR/Cas9-mediated generation of Ppm1a$^{-/-}$ cells

CRISPR/Cas9 genomic editing for gene deletion was described by Ran *et al.* (*59*). Guide RNA (gRNA) sequences targeting Ppm1a exon were cloned into the plasmid px330. Constructs together with puromycin vector were transfected into HEK293T cells by PEI. Twenty-four hours after transfection, cells were selected with puromycin (1.5 μg/ml) for another 72 hours, and single colonies were obtained by serial dilution and amplification. Clones were identified by immunoblotting with anti-PPM1A antibody, and two clones of Ppm1a$^{-/-}$ were used for the indicated analyses. gRNA sequence is listed in the Supplementary Materials.

Ectopic expression of hPPM1A and VSV challenge in zebrafish

We developed a system of gVSV challenge in zebrafish embryos to rapidly assess gene functions on antiviral defense. Forced expression of exogenous genes was obtained by microinjection of mRNA in the one-cell stage of embryogenesis, that is, in the first 20 min upon fertilization. At this stage, exogenous mRNAs distribute most evenly into most of the cells through cell division and last for 72 to 96 hours in zebrafish embryos (*60*, *61*). Zebrafish embryos were incubated at 28.5°C in E3 egg water. mRNA of hPPM1A and MAVS was transcribed in vitro with mMESSAGE mMACHINE SP6 Transcription Kit (Life Technologies), and 25 pg of PPM1A or MAVS mRNA was injected into AB wild-type embryos. Injected embryos with normal development were selected and used for the gVSV virus injection (1×10^3 PFU per embryo) in the embryo yolk at 48 hpf. The infection and death rates of injected embryos were measured at desired stages. To detect expression of PPM1A or MAVS by immunoblotting, desired tissue samples were homogenized and lysed in MLB and subjected to SDS-PAGE and immunoblotting. Care of experimental animals was in accordance with Zhejiang University guidelines.

Mouse VSV challenge

Six 8-week-old Ppm1a$^{-/-}$ and six wild-type C57BL/6 mice were intravenously injected through the tail vein with gVSV at a dose of 2×10^7 PFU/g (animal weight). The survival rate of injected mice was monitored at indicated stages as shown in the figures. In a parallel experiment, six Ppm1a$^{-/-}$ and six wild-type mice were injected with gVSV at a dose of 1×10^7 PFU/g, and all mice were sacrificed at 12 hpi. Organs, including liver, lung, and spleen were collected. All organs were lavaged by 1 ml of cold phosphate-buffered saline and snap-frozen in liquid nitrogen for RNA and protein extraction. Virus load was measured by qRT-PCR, with the primer targeting the VSV genome (listed in the Supplementary Materials). To assess the antiviral response to gVSV infection, four Ppm1a$^{-/-}$ and four wild-type mice were intravenously injected through the tail vein with gVSV (1×10^7 PFU/g) and sacrificed at 6 hpi. The PBMCs were isolated from animal blood using Percoll (Sigma), and mRNA expression of ISGs was analyzed by qRT-PCR. Care of experimental animals was in accordance with Zhejiang University guidelines.

Statistics

Quantitative data are presented as means ± SEM from at least three independent experiments. Data presented as either fold change or percentage were log-transformed before statistical analysis. When appropriate, statistical differences between groups were analyzed using an unpaired or paired Student's *t* test or by SigmaPlot 10.0. Differences were considered significant at $P < 0.05$.

SUPPLEMENTARY MATERIALS

Supplementary material for this article is available at http://advances.sciencemag.org/cgi/content/full/2/7/e1501889/DC1

fig. S1. Reporter screen of RLR/IRF3 pathway by human Ser/Thr phosphatase cDNAs.

fig. S2. Short hairpin RNA–mediated PPM1A depletion results in an enhanced antiviral signaling.

fig. S3. Enhanced basal expression of ISGs in Ppm1a$^{-/-}$ BMDMs.

fig. S4. Colocalization of TBK1 with endogenous PPM1A in cytosol.

fig. S5. mRNA level of PPM1A is not significantly changed in response to virus infection.

Oligo sequence of qPCR and CRISPR/Cas9

REFERENCES AND NOTES

1. S. Akira, S. Uematsu, O. Takeuchi, Pathogen recognition and innate immunity. *Cell* **124**, 783–801 (2006).
2. M. Yoneyama, K. Onomoto, M. Jogi, T. Akaboshi, T. Fujita, Viral RNA detection by RIG-I-like receptors. *Curr. Opin. Immunol.* **32**, 48–53 (2015).
3. Y. K. Chan, M. U. Gack, RIG-I-like receptor regulation in virus infection and immunity. *Curr. Opin. Virol.* **12**, 7–14 (2015).
4. X.-D. Li, J. Wu, D. Gao, H. Wang, L. Sun, Z. J. Chen, Pivotal roles of cGAS-cGAMP signaling in antiviral defense and immune adjuvant effects. *Science* **341**, 1390–1394 (2013).
5. F. Civril, T. Deimling, C. C. de Oliveira Mann, A. Ablasser, M. Moldt, G. Witte, V. Hornung, K.-P. Hopfner, Structural mechanism of cytosolic DNA sensing by cGAS. *Nature* **498**, 332–337 (2013).

6. P. Gao, P. Gao, M. Ascano, Y. Wu, W. Barchet, B. L. Gaffney, T. Zillinger, A. A. Serganov, Y. Liu, R. A. Jones, G. Hartmann, T. Tuschl, D. J. Patel, Cyclic [G(2′,5′)pA(3′,5′)p] is the metazoan second messenger produced by DNA-activated cyclic GMP-AMP synthase. *Cell* **153**, 1094–1107 (2013).
7. L. Sun, J. Wu, F. Du, X. Chen, Z. J. Chen, Cyclic GMP-AMP synthase is a cytosolic DNA sensor that activates the type I interferon pathway. *Science* **339**, 786–791 (2013).
8. A. Takaoka, Z. C. Wang, M. K. Choi, H. Yanai, H. Negishi, T. Ban, Y. Lu, M. Miyagishi, T. Kodama, K. Honda, Y. Ohba, T. Taniguchi, DAI (DLM-1/ZBP1) is a cytosolic DNA sensor and an activator of innate immune response. *Nature* **448**, 501–505 (2007).
9. Y.-H. Chiu, J. B. MacMillan, Z. J. Chen, RNA polymerase III detects cytosolic DNA and induces type I interferons through the RIG-I pathway. *Cell* **138**, 576–591 (2009).
10. L. Unterholzner, S. E. Keating, M. Baran, K. A. Horan, S. B. Jensen, S. Sharma, C. M. Sirois, T. Jin, E. Latz, T. S. Xiao, K. A. Fitzgerald, S. R. Paludan, A. G. Bowie, IFI16 is an innate immune sensor for intracellular DNA. *Nat. Immunol.* **11**, 997–1004 (2010).
11. Z. Zhang, B. Yuan, M. Bao, N. Lu, T. Kim, Y.-J. Liu, The helicase DDX41 senses intracellular DNA mediated by the adaptor STING in dendritic cells. *Nat. Immunol.* **12**, 959–965 (2011).
12. S. Sharma, B. R. tenOever, N. Grandvaux, G.-P. Zhou, R. Lin, J. Hiscott, Triggering the interferon antiviral response through an IKK-related pathway. *Science* **300**, 1148–1151 (2003).
13. K. A. Fitzgerald, S. M. McWhirter, K. L. Faia, D. C. Rowe, E. Latz, D. T. Golenbock, A. J. Coyle, S.-M. Liao, T. Maniatis, IKKε and TBK1 are essential components of the IRF3 signaling pathway. *Nat. Immunol.* **4**, 491–496 (2003).
14. T. Kawai, K. Takahashi, S. Sato, C. Coban, H. Kumar, H. Kato, K. J. Ishii, O. Takeuchi, S. Akira, IPS-1, an adaptor triggering RIG-I- and Mda5-mediated type I interferon induction. *Nat. Immunol.* **6**, 981–988 (2005).
15. L.-G. Xu, Y.-Y. Wang, K.-J. Han, L.-Y. Li, Z. Zhai, H.-B. Shu, VISA is an adapter protein required for virus-triggered IFN-β signaling. *Mol. Cell* **19**, 727–740 (2005).
16. R. B. Seth, L. Sun, C.-K. Ea, Z. J. Chen, Identification and characterization of MAVS, a mitochondrial antiviral signaling protein that activates NF-κB and IRF3. *Cell* **122**, 669–682 (2005).
17. E. Meylan, J. Curran, K. Hofmann, D. Moradpour, M. Binder, R. Bartenschlager, J. Tschopp, Cardif is an adaptor protein in the RIG-I antiviral pathway and is targeted by hepatitis C virus. *Nature* **437**, 1167 (2005).
18. F. Hou, L. Sun, H. Zheng, B. Skaug, Q.-X. Jiang, Z. J. Chen, MAVS forms functional prion-like aggregates to activate and propagate antiviral innate immune response. *Cell* **146**, 448–461 (2011).
19. T. Kawasaki, T. Kawai, S. Akira, Recognition of nucleic acids by pattern-recognition receptors and its relevance in autoimmunity. *Immunol. Rev.* **243**, 61–73 (2011).
20. S. M. Belgnaoui, S. Paz, J. Hiscott, Orchestrating the interferon antiviral response through the mitochondrial antiviral signaling (MAVS) adapter. *Curr. Opin. Immunol.* **23**, 564–572 (2011).
21. B. Zhong, Y. Zhang, B. Tan, T.-T. Liu, Y.-Y. Wang, H.-B. Shu, The E3 ubiquitin ligase RNF5 targets virus-induced signaling adaptor for ubiquitination and degradation. *J. Immunol.* **184**, 6249–6255 (2010).
22. F. You, H. Sun, X. Zhou, W. Sun, S. Liang, Z. Zhai, Z. Jiang, PCBP2 mediates degradation of the adaptor MAVS via the HECT ubiquitin ligase AIP4. *Nat. Immunol.* **10**, 1300–1308 (2009).
23. X.-D. Li, L. Sun, R. B. Seth, G. Pineda, Z. J. Chen, Hepatitis C virus protease NS3/4A cleaves mitochondrial antiviral signaling protein off the mitochondria to evade innate immunity. *Proc. Natl. Acad. Sci. U.S.A.* **102**, 17717–17722 (2005).
24. S. Liu, X. Cai, J. Wu, Q. Cong, X. Chen, T. Li, F. Du, J. Ren, Y.-T. Wu, N. V. Grishin, Z. J. Chen, Phosphorylation of innate immune adaptor proteins MAVS, STING, and TRIF induces IRF3 activation. *Science* **347**, aaa2630 (2015).
25. S. H. Schilling, M. B. Datto, X.-F. Wang, A phosphatase controls the fate of receptor-regulated Smads. *Cell* **125**, 838–840 (2006).
26. M. Takekawa, T. Maeda, H. Saito,Protein phosphatase 2Cα inhibits the human stress-responsive p38 and JNK MAPK pathways. *EMBO J.* **17**, 4744–4752 (1998).
27. A. Cheng, K. E. Ross, P. Kaldis, M. J. Solomon, Dephosphorylation of cyclin-dependent kinases by type 2C protein phosphatases. *Genes Dev.* **13**, 2946–2957 (1999).
28. X. Lin, X. Duan, Y.-Y. Liang, Y. Su, K. H. Wrighton, J. Long, M. Hu, C. M. Davis, J. Wang, F. C. Brunicardi, Y. Shi, Y.-G. Chen, A. Meng, X.-H. Feng, PPM1A functions as a Smad phosphatase to terminate TGFβ signaling. *Cell* **125**, 915–928 (2006).
29. F. Dai, T. Shen, Z. Li, X. Lin, X.-H. Feng, PPM1A dephosphorylates RanBP3 to enable efficient nuclear export of Smad2 and Smad3. *EMBO Rep.* **12**, 1175–1181 (2011).
30. Z. Dvashi, H. Sar Shalom, M. Shohat, D. Ben-Meir, S. Ferber, R. Satchi-Fainaro, R. Ashery-Padan, M. Rosner, A. S. Solomon, S. Lavi, Protein phosphatase magnesium dependent 1A governs the wound healing–inflammation–angiogenesis cross talk on injury. *Am. J. Pathol.* **184**, 2936–2950 (2014).
31. X. Yang, Y. Teng, N. Hou, X. Fan, X. Cheng, J. Li, L. Wang, Y. Wang, X. Wu, X. Yang, Delayed re-epithelialization in Ppm1a gene-deficient mice is mediated by enhanced activation of Smad2. *J. Biol. Chem.* **286**, 42267–42273 (2011).
32. W. Sun, Y. Yu, G. Dotti, T. Shen, X. Tan, B. Savoldo, A. K. Pass, M. Chu, D. Zhang, X. Lu, S. Fu, X. Lin, J. Yang, PPM1A and PPM1B act as IKKβ phosphatases to terminate TNFα-induced IKKβ-NF-κB activation. *Cell. Signal.* **21**, 95–102 (2009).
33. X. Lu, H. An, R. Jin, M. Zou, Y. Guo, P.-F. Su, D. Liu, Y. Shyr, W. G. Yarbrough, PPM1A is a RelA phosphatase with tumor suppressor-like activity. *Oncogene* **33**, 2918–2927 (2014).
34. Z. Li, G. Liu, L. Sun, Y. Teng, X. Guo, J. Jia, J. Sha, X. Yang, D. Chen, Q. Sun, PPM1A regulates antiviral signaling by antagonizing TBK1-mediated STING phosphorylation and aggregation. *PLOS Pathog.* **11**, e1004783 (2015).
35. M. Yoneyama, M. Kikuchi, T. Natsukawa, N. Shinobu, T. Imaizumi, M. Miyagishi, K. Taira, S. Akira, T. Fujita, The RNA helicase RIG-I has an essential function in double-stranded RNA-induced innate antiviral responses. *Nat. Immunol.* **5**, 730–737 (2004).
36. M. D. Jackson, C. C. Fjeld, J. M. Denu, Probing the function of conserved residues in the serine/threonine phosphatase PP2Cα. *Biochemistry* **42**, 8513–8521 (2003).
37. Y. Tanaka, Z. J. Chen, STING specifies IRF3 phosphorylation by TBK1 in the cytosolic DNA signaling pathway. *Sci. Signal.* **5**, ra20 (2012).
38. M. Yoneyama, T. Fujita, RNA recognition and signal transduction by RIG-I-like receptors. *Immunol. Rev.* **227**, 54–65 (2009).
39. J. Wu, L. Sun, X. Chen, F. Du, H. Shi, C. Chen, Z. J. Chen, Cyclic GMP-AMP Is an endogenous second messenger in innate immune signaling by cytosolic DNA. *Science* **339**, 826–830 (2013).
40. Y.-M. Loo, M. Gale Jr., Immune signaling by RIG-I-like receptors. *Immunity* **34**, 680–692 (2011).
41. J. Hiscott, R. Lin, P. Nakhaei, S. Paz, MasterCARD: A priceless link to innate immunity. *Trends Mol. Med.* **12**, 53–56 (2006).
42. X. Jiang, L. N. Kinch, C. A. Brautigam, X. Chen, F. Du, N. V. Grishin, Z. J. Chen, Ubiquitin-induced oligomerization of the RNA sensors RIG-I and MDA5 activates antiviral innate immune response. *Immunity* **36**, 959–973 (2012).
43. S. Liu, J. Chen, X. Cai, J. Wu, X. Chen, Y.-T. Wu, L. Sun, Z. J. Chen, MAVS recruits multiple ubiquitin E3 ligases to activate antiviral signaling cascades. *Elife* **2**, e00785 (2013).
44. W. Zeng, L. Sun, X. Jiang, X. Chen, F. Hou, A. Adhikari, M. Xu, Z. J. Chen, Reconstitution of the RIG-I pathway reveals a signaling role of unanchored polyubiquitin chains in innate immunity. *Cell* **141**, 315–330 (2010).
45. W. Zeng, M. Xu, S. Liu, L. Sun, Z. J. Chen, Key role of Ubc5 and lysine-63 polyubiquitination in viral activation of IRF3. *Mol. Cell* **36**, 315–325 (2009).
46. B. R. tenOever, S. Sharma, W. Zou, Q. Sun, N. Grandvaux, I. Julkunen, H. Hemmi, M. Yamamoto, S. Akira, W.-C. Yeh, R. Lin, J. Hiscott, Activation of TBK1 and IKKε kinases by vesicular stomatitis virus infection and the role of viral ribonucleoprotein in the development of interferon antiviral immunity. *J. Virol.* **78**, 10636–10649 (2004).
47. Y. Zhao, L. Liang, Y. Fan, S. Sun, L. An, Z. Shi, J. Cheng, W. Jia, W. Sun, Y. Mori-Akiyama, H. Zhang, S. Fu, J. Yang, PPM1B negatively regulates antiviral response via dephosphorylating TBK1. *Cell. Signal.* **24**, 2197–2204 (2012).
48. H. An, J. Hou, J. Zhou, W. Zhao, H. Xu, Y. Zheng, Y. Yu, S. Liu, X. Cao, Phosphatase SHP-1 promotes TLR- and RIG-I-activated production of type I interferon by inhibiting the kinase IRAK1. *Nat. Immunol.* **9**, 542–550 (2008).
49. E. Wies, M. K. Wang, N. P. Maharaj, K. Chen, S. Zhou, R. W. Finberg, M. U. Gack, Dephosphorylation of the RNA sensors RIG-I and MDA5 by the phosphatase PP1 is essential for innate immune signaling. *Immunity* **38**, 437–449 (2013).
50. A. W. Mesman, E. M. Zijlstra-Willems, T. M. Kaptein, R. L. de Swart, M. E. Davis, M. Ludlow, W. P. Duprex, M. U. Gack, S. I. Gringhuis, T. B. H. Geijtenbeek, Measles virus suppresses RIG-I-like receptor activation in dendritic cells via DC-SIGN-mediated inhibition of PP1 phosphatases. *Cell Host Microbe* **16**, 31–42 (2014).
51. Z. Zhan, H. Cao, X. Xie, L. Yang, P. Zhang, Y. Chen, H. Fan, Z. Liu, X. Liu, Phosphatase PP4 negatively regulates type I IFN production and antiviral innate immunity by dephosphorylating and deactivating TBK1. *J. Immunol.* **195**, 3849–3857 (2015).
52. W. Chen, J. Wu, L. Li, Z. Zhang, J. Ren, Y. Liang, F. Chen, C. Yang, Z. Zhou, S. S. Su, X. Zheng, Z. Zhang, C.-Q. Zhong, H. Wan, M. Xiao, X. Lin, X.-H. Feng, J. Han, Ppm1b negatively regulates necroptosis through dephosphorylating Rip3. *Nat. Cell Biol.* **17**, 434–444 (2015).
53. L. Long, Y. Deng, F. Yao, D. Guan, Y. Feng, H. Jiang, X. Li, P. Hu, X. Lu, H. Wang, J. Li, X. Gao, D. Xie, Recruitment of phosphatase PP2A by RACK1 adaptor protein deactivates transcription factor IRF3 and limits type I interferon signaling. *Immunity* **40**, 515–529 (2014).
54. A. Cáceres, B. Perdiguero, C. E. Gómez, M. V. Cepeda, C. Caelles, C. O. Sorzano, M. Esteban, Involvement of the cellular phosphatase DUSP1 in vaccinia virus infection. *PLOS Pathog.* **9**, e1003719 (2013).
55. J.-G. Zhang, D. Metcalf, S. Rakar, M. Asimakis, C. J. Greenhalgh, T. A. Willson, R. Starr, S. E. Nicholson, W. Carter, W. S. Alexander, D. J. Hilton, N. A. Nicola, The SOCS box of suppressor of cytokine signaling-1 is important for inhibition of cytokine action in vivo. *Proc. Natl. Acad. Sci. U.S.A.* **98**, 13261–13265 (2001).
56. P. Xu, S. Bailey-Bucktrout, Y. Xi, D. Xu, D. Du, Q. Zhang, W. Xiang, J. Liu, A. Melton, D. Sheppard, H. A. Chapman, J. A. Bluestone, R. Derynck, Innate antiviral host defense attenuates TGF-β function through IRF3-mediated suppression of Smad signaling. *Mol. Cell* **56**, 723–737 (2014).

57. P. Xu, R. Derynck, Direct activation of TACE-mediated ectodomain shedding by p38 MAP kinase regulates EGF receptor-dependent cell proliferation. *Mol. Cell* **37**, 551–566 (2010).
58. C. Ding, D. W. Chan, W. Liu, M. Liu, D. Li, L. Song, C. Li, J. Jin, A. Malovannaya, S. Y. Jung, B. Zhen, Y. Wang, J. Qin, Proteome-wide profiling of activated transcription factors with a concatenated tandem array of transcription factor response element. *Proc. Natl. Acad. Sci. U.S.A.* **110**, 6771–6776 (2013).
59. F. A. Ran, P. D. Hsu, J. Wright, V. Agarwala, D. A. Scott, F. Zhang, Genome engineering using the CRISPR-Cas9 system. *Nat. Protoc.* **8**, 2281–2308 (2013).
60. D. Beis, D. Y. R. Stainier, In vivo cell biology: Following the zebrafish trend. *Trends Cell Biol.* **16**, 105–112 (2006).
61. F. Xiong, W. Ma, T. W. Hiscock, K. R. Mosaliganti, A. R. Tentner, K. A. Brakke, N. Rannou, A. Gelas, L. Souhait, I. A. Swinburne, N. D. Obholzer, S. G. Megason, Interplay of cell shape and division orientation promotes robust morphogenesis of developing epithelia. *Cell* **159**, 415–427 (2014).

Acknowledgments: We are grateful to J. Han for the HSV-1–GFP-Luc virus and Y. Huang and J. Liu for the reagents and technical assistance. **Funding:** This research was sponsored by Chinese Ministry of Science and Technology (MOST) 973 Program (2015CB553800 to P.X.), MOST Major Program (2012CB966600 to X.-H.F.), National Natural Science Foundation of China grants (81472665 to P.X., 91540205 and 31571447 to X.-H.F.), Project 111 (to X.-H.F.), Project 985, and the Fundamental Research Funds for the Central Universities (to the Life Sciences Institute at Zhejiang University). P.X. is a scholar of the National 1000 Young Talents Program. **Author contributions:** P.X. and X.-H.F. conceived the study and experimental design and wrote the manuscript. W.X. and Q.Z. carried out most of the experiments. X.L., S.W., Y.Z., F.M., Y.F., T.S., M.X., Z.X., and J.Z. contributed to several experiments or helped with data analyses and through discussions. **Competing interests:** The authors declare that they have no competing interests. **Data and materials availability:** All data needed to evaluate the conclusions in the paper are present in the paper and/or the Supplementary Materials. Additional data related to this paper may be requested from the authors.

Submitted 24 December 2015
Accepted 31 May 2016
Published 1 July 2016
10.1126/sciadv.1501889

Citation: W. Xiang, Q. Zhang, X. Lin, S. Wu, Y. Zhou, F. Meng, Y. Fan, T. Shen, M. Xiao, Z. Xia, J. Zou, X.-H. Feng, P. Xu, PPM1A silences cytosolic RNA sensing and antiviral defense through direct dephosphorylation of MAVS and TBK1. *Sci. Adv.* **2**, e1501889 (2016).

ScienceAdvances
AAAS

PPM1A silences cytosolic RNA sensing and antiviral defense through direct dephosphorylation of MAVS and TBK1

Weiwen Xiang, Qian Zhang, Xia Lin, Shiying Wu, Yao Zhou, Fansen Meng, Yunyun Fan, Tao Shen, Mu Xiao, Zongping Xia, Jian Zou, Xin-Hua Feng and Pinglong Xu (July 1, 2016)

Sci Adv 2016, 2:.
doi: 10.1126/sciadv.1501889